STABILIZATION OF GAS-FILLED SURGE ARRESTER'S CHARACTERISTICS BY USE OF IONIZING RADIATION

by

***Dragan V. BRAJOVIĆ*[1], *Miloš Lj. VUJISIĆ*[1], *Mirko N. STOJKANOVIĆ*[1], *Uroš D. KOVAČEVIĆ*[1], *and Aleksandra I. VASIĆ*[2]**

[1]Faculty of Electrical Engineering, University of Belgrade, Belgrade, Serbia
[2]Faculty of Mechanical Engineering, University of Belgrade, Belgrade, Serbia

Scientific paper
DOI: 10.2298/NTRP1203274B

This paper investigates the stabilization of electrical discharges in gases by means of external ionizing radiation. Discharges in a gas-filled surge arrester model were studied in both passive and active regimes of the device. An originally developed model of the gas-filled surge arrester was used. Gas pressure and the interelectrode gap were the variable parameters in our measurements. Applied radiation types included α-particles, γ-rays, X-rays, and neutrons. Measurements were performed under highly controlled laboratory conditions. The combined measurement uncertainty of the applied procedure was estimated as being under the 5% level. The results obtained are followed by a theoretical explanation. The crucial result is the conclusion that ionizing radiation does not necessarily degrade the gas-filled surge arrester's functionality but that it, rather, improves it under certain conditions.

Key words: passive and active properties, gas-filled surge arresters, ionizing radiation, neutron radiation

INTRODUCTION

Sensitivity to overvoltage increases significantly with component miniaturization. Reliable overvoltage protection of modern electronic devices is, therefore, of major importance. If the devices are not properly protected against overvoltage, components can suffer damages leading to partial or complete destruction [1].

Overvoltage components are either linear or nonlinear. Linear overvoltage protection components include various types of filters consisting of coils and capacitors. Non-linear overvoltage protection components include gas-filled surge arresters (GFSA), metal-oxide varistors (MOV), and transient suppressor diodes (TSD) [2]. GFSA are made of a glass or ceramic housing, with a gas-insulated symmetrical two- or three-electrode configuration. Noble gases at pressures close to the Paschen minimum are mostly used for insulation [3]. The operation of a GFSA rests upon the electrical breakdown of the insulating gas. The breakdown is a consequence of a self-sustained avalanche process which depends on the competition of electron generation and loss processes [4, 5]. The advantages of a GFSA over other overvoltage protection components are its ability to conduct high currents (up to 5000 A), its low intrinsic capacity (~1 pF), and low cost, while its drawbacks are the irreversibility of properties after an electric arc [6-9].

Radiation environments that require proper functioning of electronic devices are diverse. For instance, a nuclear explosion produces a strong pulse of gamma rays that lasts several nanoseconds and a delayed pulse of fast neutrons that lasts several hundreds of microseconds. Depending on the type of nuclear explosions (surface, air, or high-altitude bursts), other kinds of ionizing radiation can also appear, such as the secondary γ pulse in the air, or high-altitude bursts. In nuclear power plant devices – continuous and pulse nuclear reactors – the process of fission is accompanied by the generation of neutron and gamma ($n + \gamma$) radiation. In research circles, there is a widespread use of modelling devices: continuous and pulse nuclear reactors, pulse Roentgen and γ devices, continuous γ devices, pulse and continuous electron and proton accelerators. Space is a natural environment for various radiation sources: galactic radiation (protons, alpha particles, and other heavy nuclei), solar radiation (especially during periods of high solar activity), as well as radiation from the Earth's radiation belts. This short review of radiation environments and sources illustrates the diversity of radiation conditions and factors

* Corresponding author; e-mail: vujsa@ikomline.net

that affect electronic devices in actual operating conditions.

Since it is necessary to provide reliable protection for the electronic devices from the effects of transients (such as the electromagnetic pulse following a high-altitude nuclear burst) in above mentioned conditions, the influence of ionizing radiation on gas-filled surge arresters needs to be investigated.

The aim of this paper is to examine the effects of ionizing radiation on the stability of volt-ampere and volt-second characteristics of components with gas insulation, performing in short time intervals.

EXPERIMENT

The operation of a GFSA is based on the mechanism of gas pulse breakdown which is characterized by the same order of magnitude of time constants describing the applied voltage change and elementary gas discharge processes. The value of the pulse breakdown voltage is, therefore, a stochastic quantity, which also makes the properties of a GFSA stochastic. Since the stochasticity of the pulse breakdown voltage random variable arises mainly from the stochasticity of the initiatory electron appearance [10-12], it is to be expected that a rise in the number of free electrons (potentially initiatory ones) stabilizes GFSA's characteristics.

The investigated GFSA model, consisting of a gas chamber and an electrode system that provide a homogeneous electric field, is presented in fig. 1. The gas chamber was connected to a gas circuit shown in fig. 2. Both the chamber and the gas circuit were designed to provide stable gas pressure during each series of measurements. A Walace & Tiermon Dipon 2 digital instrument, with 0.1 mbar resolution, was used

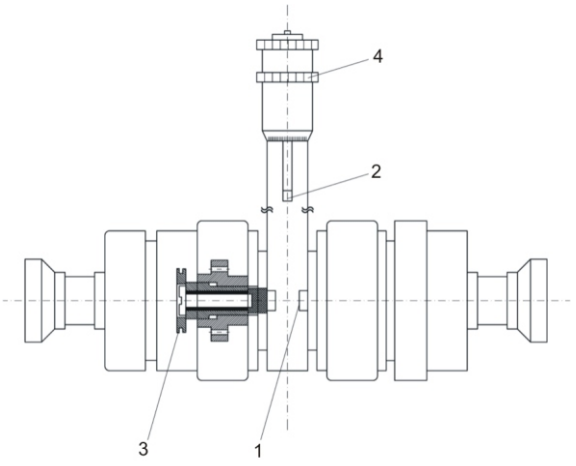

Figure 1. The GFSA mode (gas chamber and electrode system); 1 – electrode system, 2 – radioactive source carrier, 3 – fitting the interelectrode gap, 4 – fitting the distance between the radioactive source and the interelectrode gap

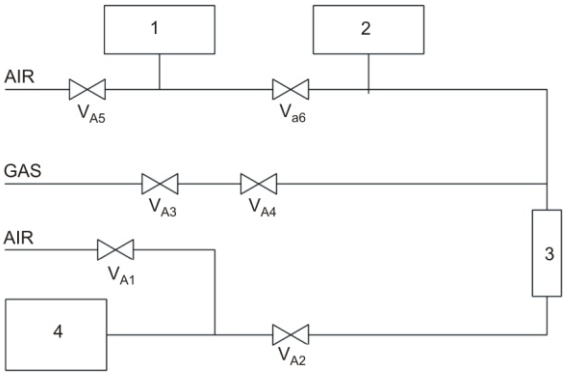

Figure 2. The scheme of the gas circuit; 1 – absolute instrument, 2 – relative instrument, 3 – chamber, 4 – vacuum pump, V_{A1}, V_{A2}, V_{A3}, V_{A5}, and V_{A6} are two-position valves, and V_{A4} is a micrometer dosing valve

for monitoring the value of the pressure inside the chamber. Measurements were recorded with a Dipon 2 and then configured by the FA-129 device of the same manufacturer. The constancy of the set pressure throughout each measurement was achieved by suitable valves.

A collimated ^{241}Am α particle source, moveable along the radial direction, was installed at the opposite side of the interelectrode gap. Its position was adapted during the experiment, so that the maximum of the Bragg curve (relative specific ionization *vs*. range, *e*. *g*. the number of created electron-ion pairs *vs*. the distance from the radioactive source) [13, 14] for any set pressure, was located at the centre of the interelectrode region. The Bragg curve maximum marked the exact position at which α particles created a maximum number of electron-ion pairs [15]

The gamma radiation field used for testing the GFSA model was a ^{60}Co field, with average gamma ray energy of 1.25 MeV. The absorbed dose rate in the air was 96 cGy/h, 960 cGy/h, and 1920 cGy/h. The distance between the radioactive source and the examined over-voltage components was 272 cm, 86 cm, and 60 cm, respectively, for the three dose rates.

X-rays used in our experiments were obtained from the Philips MG-320 X-ray generator, set to following values of parameters: the high voltage for narrow spectra was 300 kV, average energy 250 keV, electric current 15 mA. Three different filters were used, resulting in X-ray energies of 45 keV, 115 keV, and 250 keV.

Noble gas Ar was used as a filling. Pressure was varied from 1 mbar to 2.5 mbar, the interelectrode gap from 0.1 to 2 mm. The applied voltage had a 8 V/s rate of rise in the case of the DC load, and a 1.2 kV/50 μs waveform in the case of the pulse voltage load. A block diagram of the measuring system is to be found in [16].

In order to examine the effects of neutron radiation on the GFSA model, it was exposed to the radiation of a ^{252}Cf neutron source [17] that has a peak in the

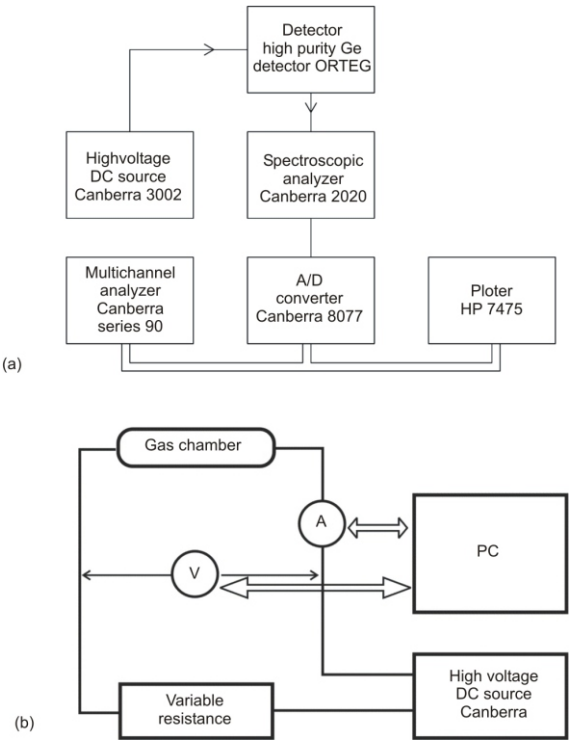

Figure 3. Block diagram of the apparatus for activation analysis (a); block diagram of the test circuit for measuring the dependence of the pre-breakdown current on the voltage (b)

neutron spectrum at the energy of 0.8 MeV, while the spectrum extends to 20 MeV.

The analysis of the γ-spectrum, arising from the isotopes created during neutron irradiation of the GFSA model, was performed with the apparatus represented by the block diagram in fig. 3(a).

The measuring equipment consisted of: (1) a gas-vacuum chamber, (2) pressure gauge SPEEDIVAC, (3) steel cylinder with Ar gas under pressure, (4) vacuum pump EDWARDS 5, (5) DC high-voltage source CANBERRA, (6) AVO meter ISKRA MI 7006, (7) digital multimeter LDM – 852 A, (8) variable resistance MA 2110, and (9) coaxial cables and connectors.

The experimental procedure was comprised of following steps: (1) assembling the GFSA model by placing the electrodes inside the gas-vacuum chamber and adjusting the interelectrode distance; (2) connecting the gas chamber to the gas-vacuum system (via suitable valves, with a vacuum pump on one side and a gas supply from a steel gas cylinder on the other), as well as to the pressure gauge; (3) vacuuming the system and establishing a stable pressure by using valves leading to the vacuum pump and valves for fine tuning; (4) positioning the gas chamber at the exact spot corresponding to the desired absorbed dose rate, *i. e.* positioning the α source at an appropriate distance, so as to locate the Bragg peak within the interelectrode region; (5) connecting the GFSA model to the electric circuit; (6) conditioning the electrode system by keeping it in the discharging state for a period of time, in order to obtain stable operating conditions that insure the repeatability of measured results; (7) measuring the pre-breakdown current as the applied voltage is being gradually increased; (8) conditioning the electrode system with 50 consecutive electric arc breakdowns, (9) measuring 1000 consecutive pulse breakdown voltages with a 1 kV/μs load voltage rate of rise, (10) measuring 20 consecutive dc breakdown voltages with a 8 kV/μs load voltage rate of rise; (11) changing experimental conditions (interelectrode gap, gas pressure, α source position, dose of γ and X-rays). The block diagram of the test circuit for measuring the dependence of pre-breakdown current on voltage is shown in fig. 3(b), while fig. 4 shows a block diagram of the test circuit for determining the values of random variables dc and pulse breakdown voltage and a simplified diagram of the output circuit.

Measurements for determining random variables dc and the pulse breakdown voltage of the GFSA model by using the test circuit represented in the block diagram, fig. 4(a), started with the PC selecting, (via a D/A converter), the appropriate working mode (cur-

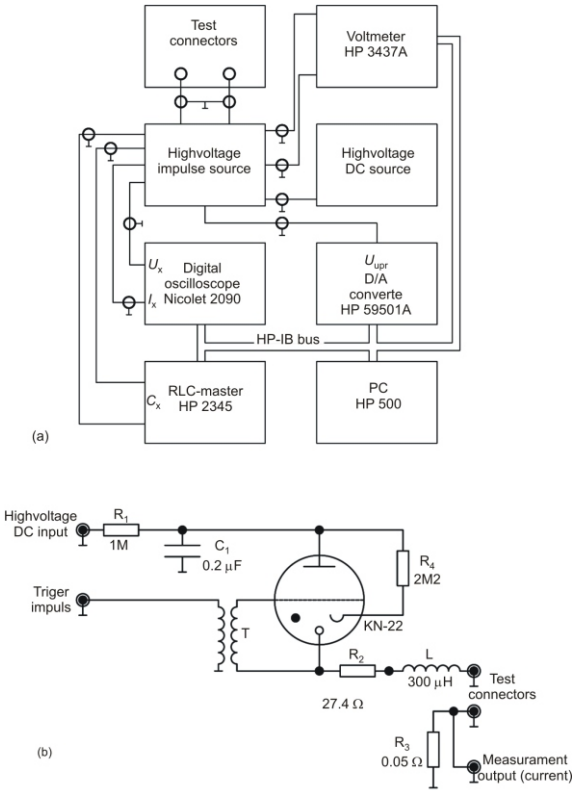

Figure 4. Block diagram of the test circuit for determining the values of random variables DC and pulse breakdown voltage (a); simplified diagram of the current impulse forming circuit (b)

rent source) whose output circuit for current impulse formation is represented in simplified form by the diagram in fig. 4(b). After the selection comes the setting of the voltage at a high DC voltage source output, followed by the charging of the capacitor C_1. After that, the KN-22 krytron is triggered (a cold-cathode gas-filled tube, used as a high-speed), forming the voltage impulse through the circuit comprised of C_1, R_2, and L. The signal from the voltage probe is then fed to the digital oscilloscope and, further on, to the PC for processing. The procedure is then repeated. DC (static) testing of the GFSA model was conducted with a unipolar load voltage with a 8 kV/μs rate of rise.

The procedure of processing experimental results comprised: (1) plotting the pre-breakdown current against voltage by means of dose, energy and type of radiation as variable parameters; (2) eliminating spurious results from the statistical sample of the pulse breakdown voltage random variable by using Chauvenet's criterion [18]; (3) plotting volt-second characteristics by using the Area Law for an equal radiation dose, gas pressure and interelectrode gap as parameters [19]; (4) testing if the experimentally obtained results, with or without radiation, belong to an unique statistical distribution, by means of the U-test [18-21].

RESULTS AND DISCUSSION

Influence of radiation on volt-ampere characteristics

Figures 5, 6, and 7 show the volt-ampere characteristics obtained at different values of gas pressure and interelectrode gap, with the Bragg peak position and the doses of γ-rays, X-rays, or α radiation as parameters, respectively.

Figure 8 shows the dependencies of the pre-breakdown current on the applied voltage without neutron radiation, during neutron irradiation, as well as 1000 s, 4252 s, and 100000 s after irradiation.

The common feature of the Results in figs. 5, 6, 7, and 8 is that the position of the curve's saturation plateau and the voltage value at which the avalanche multiplication of ion-electron pairs is established depends on the type of radiation, its intensity and deposited dose. Figure 5 shows that the increase of the saturation plateau (I = const) at low values of the interelectrode gap and smaller gas pressures is more prominent. Under the same conditions, it is evident that the earlier appearance of multiplicative processes doesn't depend on the interelectrode gap and gas pressure. This effect can be explained by a lower concentration of free, potentially initiating electrons, in the interelectrode area when the interelectrode gap is small and pressure value low. For this reason, the effect of ionization by γ-radiation significantly increases

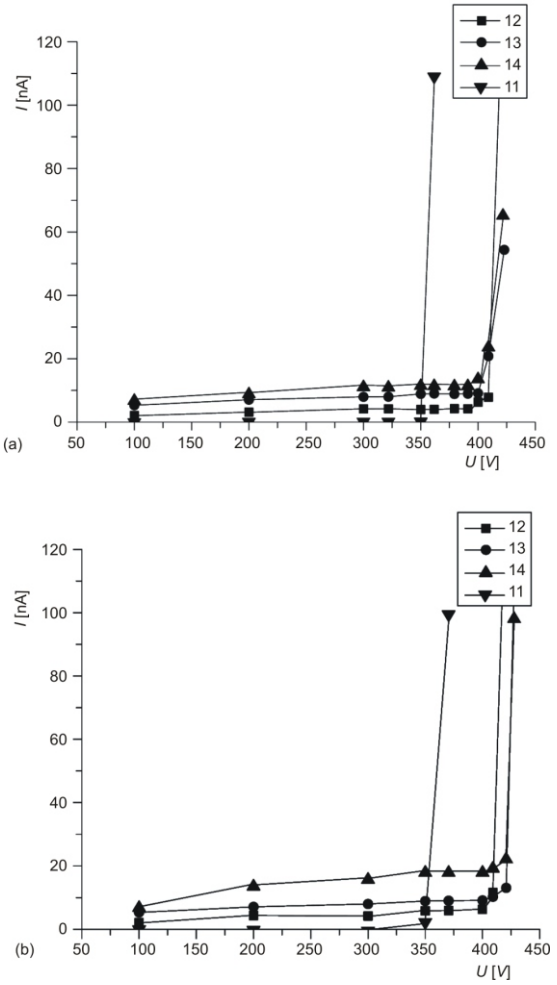

Figure 5. Pre-breakdown current versus applied voltage in the g ray field (I_1 = no radiation, I_2 = 0.96 Gy/h, I_3 = 9.6 Gy/h, and I_4 = 19.2 Gy/h); (a) interelectrode gap 0.5 mm, pressure 60 mbar; (b) interelectrode gap 0.1 mm, pressure 300 mbar

the number of available ion-electron pairs, resulting in a higher saturation level. This effect is less noticeable in the case of larger interelectrode gaps and higher pressure values. Despite the differences in the saturation level position, the multiplicative process occurs in a similar way, regardless of the interelectrode gap and gas pressure. This is due to the absorption of high radiation doses causing a rise of kinetic energy of free ionization carriers, which results in avalanche ionization beginning at lower voltages for higher doses.

Influence of radiation on volt-second characteristics

Figure 9 shows volt-second characteristics corresponding to 0.1% and 99.9% probability quantiles, obtained by using the Area Law [19], the experimentally determined dc breakdown voltage, and the statistical sample of the pulse breakdown voltage random

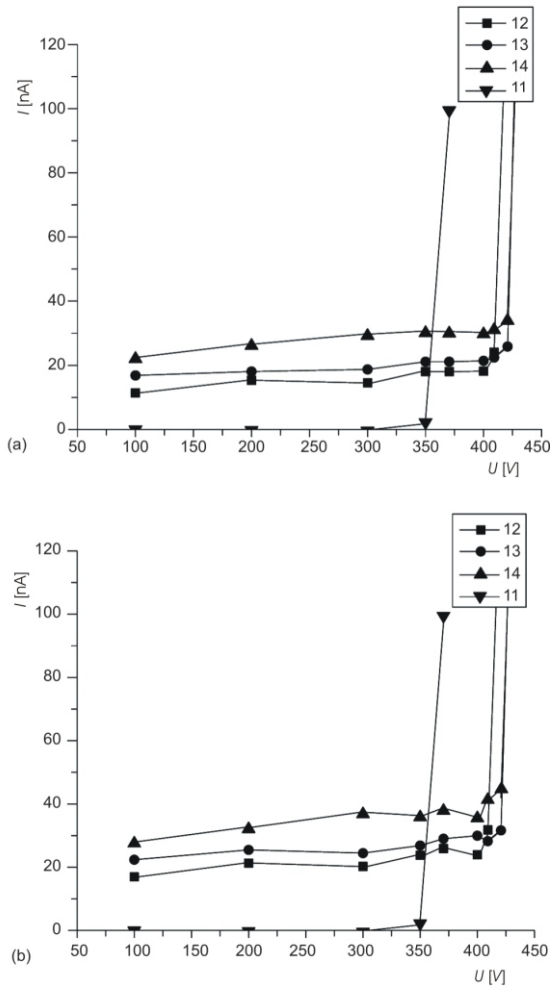

Figure 6. Pre-breakdown current *vs.* applied voltage in the X-ray field (I_1 = no radiation, I_2 = 45 keV, I_3 = 115 keV, and I_4 = 250 keV); (a) interelectrode gap 0.5 mm, pressure 60 mbar; (b) interelectrode gap 0.1 mm, pressure 300 mbar

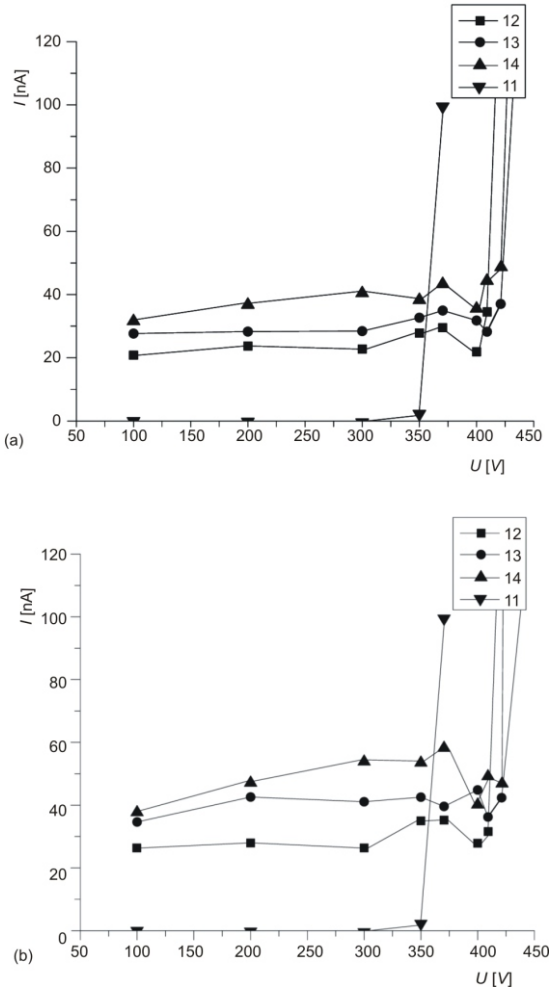

Figure 7. Pre-breakdown current *vs.* applied voltage in α the X-ray field (I_1 = no radiation, I_2 = 45 keV, I_3 = 115 keV, and I_4 = 250 keV), (a) interelectrode gap 0.5 mm, pressure 60 mbar; (b) interelectrode gap 0.1 mm, pressure 300 mbar

variable for load voltages with a 1 kV/μs rate of rise, for the non-irradiated surge arrester, surge arrester irradiated by γ-rays, as well as those irradiated by X-rays.

Results obtained in fig. 9 show that the effects of radiation lead to a narrowing of volt-second characteristics, *i. e.* their improvement in regarding practical applications. Narrower volt-second characteristics indicate a lesser dispersion of the impulse breakdown voltage random variable which is of considerable importance for predicting the behaviour of gas filled surge arresters in practice. Effects of radiation also increase the number of free, potentially initiating electrons, and thereby decrease the value of the impulse breakdown voltage, bringing it close to the nominal values of the dc voltage. As can be seen from fig. 9, the same effect was more pronounced in the case of X-radiation than in the case of γ-radiation. This is due to the fact that X-radiation (due to its wavelengths), most often interacts with the whole atom, imparting to it the energy that often leads to ionization, while γ-radiation, (due to its wavelength), reacts directly with bound electrons, causing ionization. The first process is characterized by a larger effective cross section and its effect is, therefore, more pronounced.

Figure 10 shows volt-second characteristics for the non-irradiated surge arrester, and for the surge arrester irradiated by neutrons. This figure clearly shows the narrowing of the volt-second characteristics bounded by 0.1% and 99.9% quantiles, caused by a higher probability for an ionizing particle or a γ quantum to be found in the interelectrode region.

Gamma radiation significantly affects the pre-breakdown current of the GFSA model. With no gamma source present, before the breakdown voltage is reached, the pre-breakdown current doesn't change with the rising voltage. When there is a gamma source present, there is a noticeable steady rise of the pre-breakdown current with the rise of the load voltage. The rise of the pre-breakdown current is more expressed for larger radiation doses, as well as for higher gas pressures at a constant value of the *pd* (gas pres-

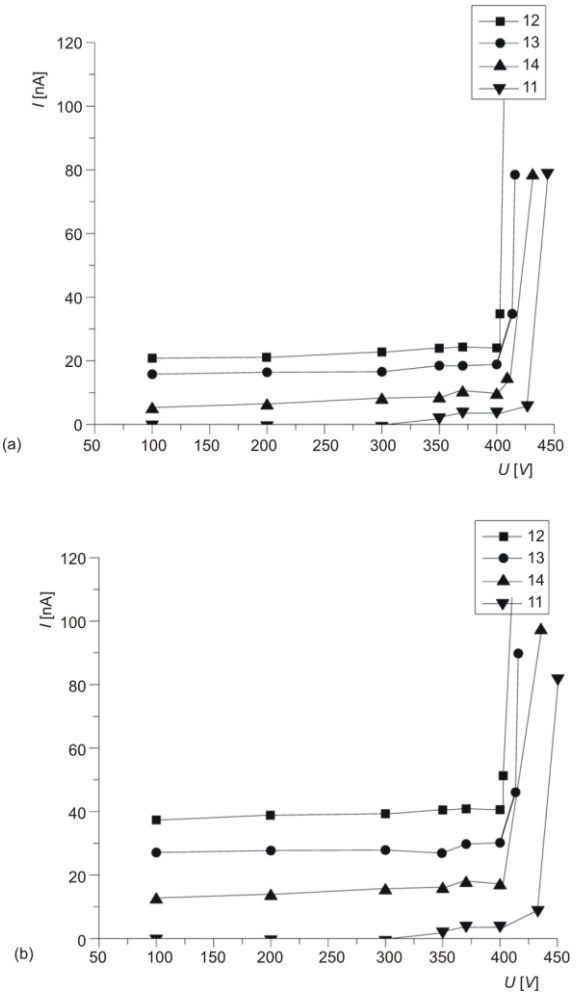

Figure 8. Pre-breakdown current *vs*. applied voltage in neutron radiation field (I_1 = no radiation, I_2 = 1000 s after irradiation, I_3 – 4252 s after irradiation, and I_4 – 100000 s after irradiation); (a) interelectrode gap 0.5 mm, gas pressure 60 mbar; (b) interelectrode gap 0.1 mm, pressure 300 mbar

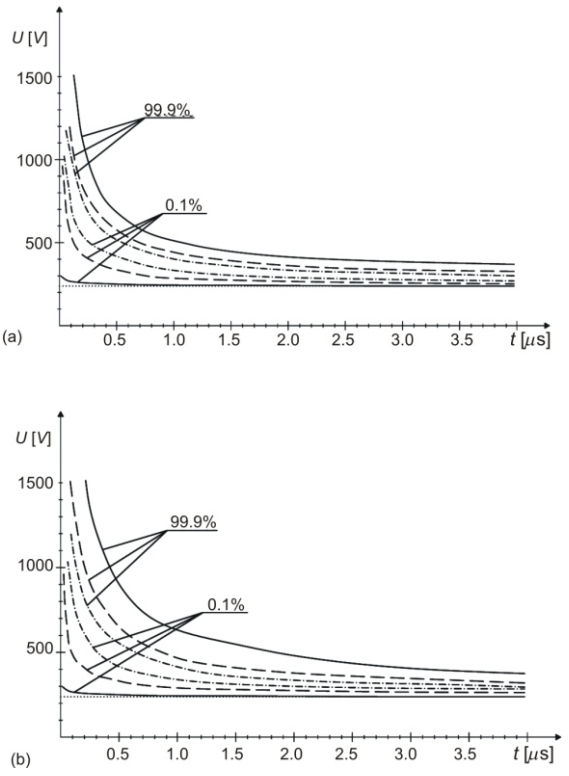

Figure 9. Volt-second characteristics without radiation (———), with a 19.2 Gy/h dose rate γ-ray field present (-----), with 250 keV X-rays present (-·-·-·-); (a) interelectrode gap 0.1 mm, gas pressure 100 mbar; (b) interelectrode gap 0.01 mm, gas pressure 1000 mbar

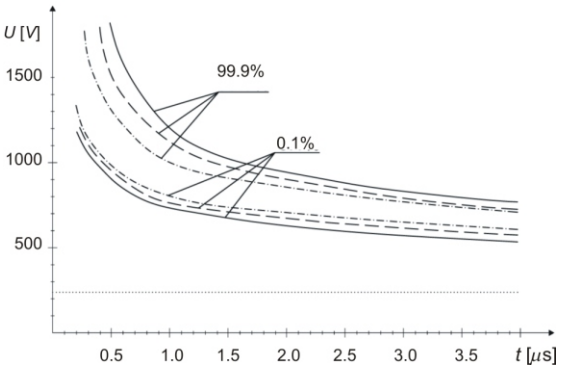

Figure 10. Volt-second characteristics of the surge arrester without irradiation (——), immediately upon neutron irradiation (----), and 30 min after neutron irradiation (-·-·-·-); interelectrode gap 0.5 mm, gas pressure 200 mbar

sure × inter-electrode gap) product. In the case of X-rays, the pre-breakdown current has a constant value that is higher for larger X-ray energies, the effect being more pronounced than when γ-rays are concerned. This can be attributed to the higher ionizing efficiency of X-rays, which, owing to the higher wavelength (commensurable to atomic dimensions) interact with an atom as a whole, transferring to it an energy higher than the electron binding energy, while γ-rays interact with individual electrons (through photoelectric or Compton effect), which makes the energy that corresponds to ionization by γ rays lower than the energy that corresponds to ionization by X-rays. Alpha radiation has the greatest influence regarding the pre-breakdown current rise. This can be explained by a much higher ionizing efficiency of á radiation, compared to X-rays and γ-rays, especially in the conditions of our experiment, *i*. *e*. when the Bragg peak is positioned within the interelectrode region. As for γ-rays and X-rays, in the case of α particle irradiation, the observed effects are much more pronounced for higher values of the pd product, *i*. *e*. when the requirement for the validity of the Similarity Law for gas discharge is fulfilled [22]. This can be explained by a shorter mean free path in case of higher pressures.

The influence of all three radiation types, (γ, X, and α), on the DC breakdown voltage value is negligible. On the other hand, the dynamic breakdown voltage, represented by the volt-second characteristics, behaves in the same manner as the pre-breakdown current. Namely, the higher the ionizing efficiency, the smaller the area in the volt-second plane limited by the 0.1% and 99.9% quantiles, which makes the gas discharge more stable. This can be explained by the shortening of statistical time [23], (*i. e*. of the interval between the advent of a free electron and its transformation into an initiatory one), caused by the increase of free electron density in the interelectrode region due to the passage of ionizing radiation.

Static load voltage tests of neutron radiation effects on the GFSA model showed that irradiation causes a significant reduction of the statistical dispersion attributed to the static breakdown voltage mean value, as a consequence of the rise of the probability for ionization process initialization, *i. e*. due to the rise of ionizing particle and γ-ray fluxes in the interelectrode region. The change of the static breakdown voltage dispersion, followed by increasing neutron fluence, is presented in fig. 11. It can be noted that the static breakdown voltage dispersion falls to a certain value after which it remains almost constant. The mean value of the static breakdown voltage remained unchanged in the irradiated GFSA model, equal to the value before irradiation.

Pulse load voltage tests performed on the GFSA model showed that it reacted more promptly after irradiation, had narrower volt-second characteristics, *i. e*. a lower dispersion of the dynamic breakdown voltage. Namely, before irradiation, the dynamic breakdown voltage dispersion was 3.11%, while after irradiation to neutron fluence of 5.4148 10^{11}neutrons/cm^2, it fell to 1.84%.

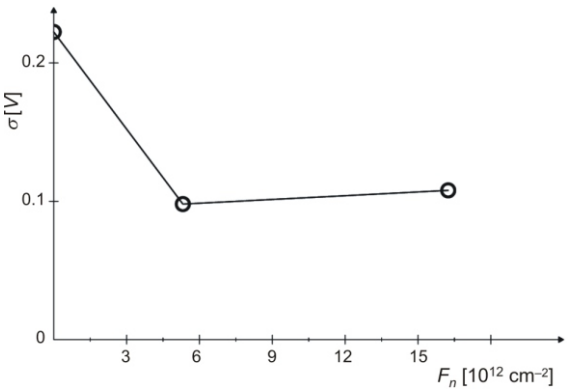

Figure 11. Change of the statistical dispersion attributed to the static breakdown voltage mean value with the rising neutron fluence

The quicker reaction of the GFSA model is caused by the shortening of statistical time that stems from the rise of the ionizing particle flux in the interelectrode region. Figure 12 presents a chronological sequence of dynamic breakdown voltage values for the non-irradiated GFSA model as a histogram, while fig. 13 shows the same characteristics for the irradiated GFSA model (F_u = 5.4148 10^{11}) neutrons/cm^2.

The differences between the chronological sequences of the dynamic breakdown voltage random variable shown in figs. 12 and 13 are a result of the ionization effect. The effect of ionization increases the number of free electrons in the interelectrode gap, significantly decreasing the dispersion of the dynamic breakdown voltage random variable. This is due to the fact that, in a homogeneous electric field, almost the entire interelectrode volume is critical, *i. e*. a space within which a free electron progressing along a mean free path can obtain enough energy from the electric field to start the avalanche process in the next collision, *i. e*. could become the initiatory electron.

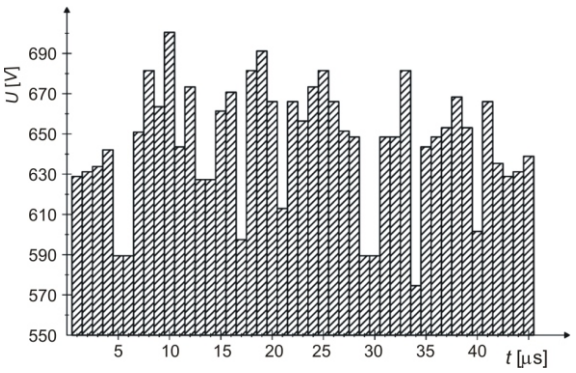

Figure 12. Chronological sequence of dynamic breakdown voltage values for the non-irradiated GFSA model

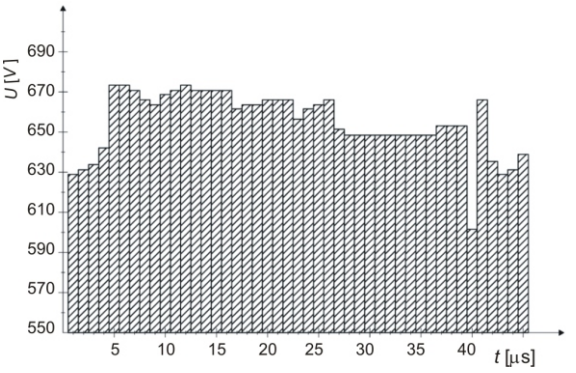

Figure 13. Chronological sequence of dynamic breakdown voltage values for the non-irradiated GFSA model

The effect of neutron radiation on the GFSA model can be explained in a similar way. Although

neutrons produce little or no direct ionization, neutron irradiation affects the characteristics of the GFSA model by activating its constructive materials, fig. 14. The radiation that comes from the deactivation of the structural materials of the GFSA only increases the number of free electrons (predominantly initiatory, due to the homogeneous geometry), leading, in turn, to the narrowing of impulse characteristics. As the activity of structural materials decreases, so does the effect of their radiation on the concentration of free electrons. Finally, it can be concluded that neutron irradiation improves the characteristics of the GFSA (by narrowing its impulse characteristics) for a period of time (determined by the half-lives of radioactive nuclei in the activated materials). This improvement is lost over time, figs. 10, 14, 15, and 16.

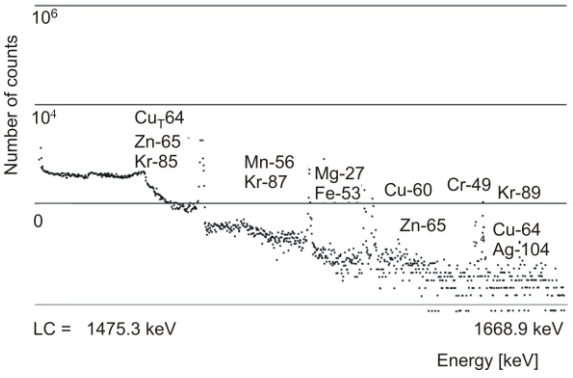

Figure 14. Results of the activation analysis performed on the GFSA model immediately after irradiation (duration of measurement: 1000 s)

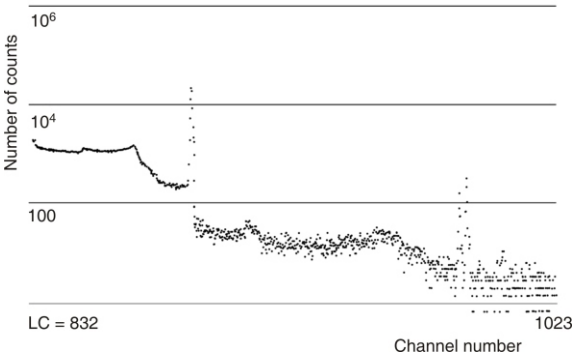

Figure 15. Results of the activation analysis performed on the GFSA model 6 hours after irradiation (duration of measurement: 4252 s)

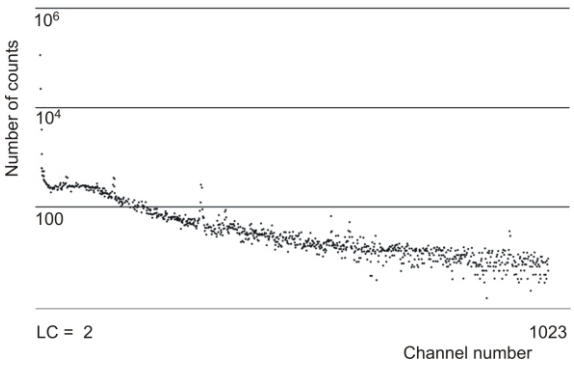

Figure 16. Background radiation measurement results for the GFSA (duration of measurement: 100000 s)

CONCLUSIONS

This paper investigates the influence of ionizing radiation fields on the properties of a gas-filled surge arrester model. Our experiments were performed with α, γ, X, and neutron radiation fields, in well-controlled laboratory conditions, with combined measurement uncertainty lower than 5%. The obtained results point to the fact that all types of ionizing radiation improve the active characteristics of the gas-filled surge arrester, while degrading its static properties. Both effects are more pronounced at higher gas pressures and smaller interelectrode gaps, with the value of the *pd* product (gas pressure × interelectrode gap) kept constant. The observed effects are most expressed for γ particle radiation, and least for γ-rays (not counting neutrons, which belong to indirectly ionizing radiation). The said effects can be explained by a higher concentration of free electrons, which are potentially initiatory, and whose presence in the interelectrode region shortens the response (*i. e*. pre-breakdown) time. This improves the active characteristics of the gas-filled surge arrester. However, the same effect (increase of free electron concentration in the interelectrode region) causes a rise in the pre-breakdown current which, for an ideal gas-filled surge arrester, should be zero. The higher efficiency of X-rays compared to γ-rays is attributed to the higher ionizing power of X-rays, which stems from their wavelength being comparable to atomic dimensions, making them react with an atom as a whole, instead of with individual electrons like γ-rays do. A similar explanation applies to the high efficiency of α-radiation, especially since the experiment was designed so that the peak of the Bragg curve was located inside the interelectrode region. Neutron effects are somewhat different. Namely, neutrons do not represent ionizing radiation directly. Their effect is seen in the activation of the gas-filled surge arrester's construction materials, which then ionizes the active gas through secondary de-excitations and increases the number of free electrons in it. The fact that these effects are more pronounced at higher gas pressures (*i. e*. higher densities) is explained by the effective cross-sections for ionization being larger in that case.

ACKNOWLEDGEMENT

The Ministry of Education and Science of the Republic of Serbia supported this work under contract 171007.

REFERENCES

[1] Shnawah, D. A., Sabri, M. F. M., Badruddin, I. A., A Review on Thermal Cycling and Drop Impact Reliability of Solder Joints in Electronic Packages, *MIDEM, 41* (2011), 3, pp. 186-192
[2] Osmokrović, P., *et al*., Radioactive Resistance of Elements for Over-Voltage Protection of Low-Voltage Systems, *Nuclear Instruments and Methods in Physics Research B, 140* (1998), 1-2, pp. 143-151
[3] Jovanović, B., *et al*., Initiation and Progress of Breakdown in the Range to the Left of the Paschen Minimum, *IEEE Transactions on Dielectrics and Electrical Insulation, 18* (2011), 4, pp. 954-963
[4] Pejović, M. M., Ristić, G. S., Karamarković, J. P., Electrical Breakdown in Low Pressure Gases, *J. Phys. D: Appl. Phys., 35* (2002), 10, pp. R91-R103
[5] Osmokrović, P., Mechanism of Electrical Breakdown of Gases at Very Low Pressure and Inter-Electrode Gap Values, *IEEE Trans. Plasma Sci., 21* (1993), 6, pp. 645-654
[6] Osmokrović, P., *et al*., Radiation Hardness of Gas Discharge Tubes and Avalanche Diodes Used for Transient Voltage Suppression, *Radiation Effects and Defects in Solids, 164* (2009), 12, pp. 800-808
[7] Osmokrović, P., Lončar, B., Stanković, S., Investigation the Optimal Method for Improvement the Protective Characteristics of Gas Filled Surge Arresters with/without the Built in Radioactive Sources, *IEEE Trans. Plasma Sci., 30* (2002), 5, pp. 1876-1880
[8] Lončar, B., Osmokrović, P., Stanković, S., Radioactive Reliability of Gas Filled Surge Arresters, *IEEE Trans. Nuclear Sci., 50* (2003), 5, pp. 1725-1731
[9] Pejović, M., Pejović, M., Stanković, K., Experimental Investigation of Breakdown Voltage and Electrical Breakdown Time Delay of Commercial Gas Discharge Tubes, *Japanese Journal of Applied Physics, 50* (2011), 8, art no. 086001
[10] Stanković, K., *et al*., Time Enlargement Law for Gas Pulse Breakdown, *Plasma Sources Science and Technology, 18* (2009), 2, 025028, p. 12
[11] Stanković, K., *et al*., Surface Time Enlargement Law for Gas Pulse Breakdown, *IEEE Transactions on Dielectrics and Electrical Insulation, 15* (2008), 4, (2008), pp. 994-1005
[12] Osmokrović, P., *et al*., Validity of the Space-Time Enlargement Law for Vacuum Breakdown, *Vacuum, 85* (2010), pp. 221-230
[13] Evans, R. D., The Atomic Nucleus, McGraw-Hill Book Company, XIII edition, New York, USA, 1970
[14] Marjanović, N., *et al*., Simulated Exposure of Titanium Dioxide Memristors to Ion Beams, *Nucl Technol Radiat, 25* (2012), 2, pp. 120-125
[15] ***, CRC Handbook of Chemistry and Physics, CRC Press, Boca Raton, Fla., USA, 1990, Editor-in-chief Robert C. Weast
[16] Lončar, B., Osmokrović, P., Stanković, S., Radioactive Reliability of Gas Filled Surge Arresters, *IEEE Trans. Nuclear Sci., 50* (2003), 5, pp. 1725-1731
[17] ***, Atomic Energy Commision: Guide for Fabricating and Handling ^{252}Cf Sources, USA, January 1971
[18] Dolićanin, Ć., *et al*., Statistisal Treatment of Nuclear Counting Results, *Nucl Technol Radiat, 26* (2011), 2, pp. 164-170
[19] Osmokrović, P., *et al*., Determination of Pulse Tolerable Voltage in Gas-Insulated Systems, *Japanese Journal of Applied Physics, 47* (2008), 12, pp. 8928-8934
[20] Stanković, K., *et al*., Statistical Analysis of the Characteristics of Some Basic Mass-Produced Passive electrical Circuits Used in Measurements, *Measurement, 4*4 (2011), 9, pp. 1713-1722
[21] Vujisić, M., Stanković, K., Osmokrović, P., A Statistical Analysis of Measurement Results Obtained from Nonlinear Physical Laws, *Applied Mathematical Modeling, 35* (2011), 7, pp. 3128-3135
[22] Osmokrović, P., *et al*., Conditions for the Applicability of the Geometrical Similarity Law to Gas Pulse Breakdown, *IEEE Transactions on Dielectrics and Electrical Insulation, 17* (2012), 4, pp. 1185-1195
[23] Stanković, K., Influence of the Plain-Parallel Electrode Surface Dimensions on the Type A Measurement Uncertainty of GM Counter, *Nucl Technol Radiat, 26* (2011), 1, pp. 39-44

Received on March 3, 2012
Accepted on July 16, 2012

Драган В. БРАЈОВИЋ, Милош Љ. ВУЈИСИЋ, Мирко Н. СТОЈКАНОВИЋ
Урош Д. КОВАЧЕВИЋ, Александра И. ВАСИЋ

СТАБИЛИЗАЦИЈА КАРАКТЕРИСТИКА ГАСНИХ ОДВОДНИКА ПРЕНАПОНА ПРИМЕНОМ ЈОНИЗУЈУЋЕГ ЗРАЧЕЊА

У раду се разматра стабилизација електричног пражњења у гасовима применом спољашњег јонизујућег зрачења. Разматрано је пражњење модела гасног одводника пренапона у пасивном и активном радном режиму. Коришћен је оригинално развијен модел гасног одводника пренапона. Параметри мерења су били притисак гаса и међуелектродно растојање. Примењено зрачење је било: α-зрачење, γ-зрачење, X-зрачење и неутронско зрачење. Мерења су вршена под добро контролисаним лабораторијским условима. Комбинована мерна несигурност примењеног поступка процењена је на мање од 5%. Добијеним резултатима је дато теоријско тумачење. Основни резултат је да јонизујуће зрачење не мора нужно да ограничава функцију гасних одводника пренапона, већ да је, под одређеним условима, побољшава.

Кључне речи: пасивне и активне карактеристике, гасни одводници пренапона, јонизујуће зрачење, неутронско зрачење